Mem. S.A.It. Suppl. Vol. 22, 110

Memorie della
Supplementi

Lithium in globular clusters: significant systematics

Atomic diffusion, the temperature scale, and pollution in NGC 6397

T. Nordlander[1], A. J. Korn[1], O. Richard[2], and K. Lind[3]

[1] Department of Physics and Astronomy, Division of Astronomy and Space Physics, Uppsala University, Box 516, 75120, Uppsala, Sweden
e-mail: Thomas.Nordlander@gmail.com
[2] LUPM, Université Montpellier 2, CNRS, place Eugène Bataillon, 34095 Montpellier, France
[3] Max-Planck-Institut für Astrophysik, Karl-Schwarzschild-Strasse 1, 857 41, Garching bei München, Germany

Abstract. We describe our latest investigation of stars in NGC 6397, as an update to Korn et al. There, effects of atomic diffusion were found to significantly affect surface abundances of lithium, as well as iron and magnesium.
In this updated analysis, we have adopted a new, hotter, temperature scale. Additionally, we now analyze lithium in NLTE, have added chromium in NLTE to the analysis, and corrected magnesium abundances for effects of cluster-internal pollution. We determine abundances in six chemical elements. Significant evolutionary variations on the 3σ level are still identified in the iron abundances. Variations in all six elements match model predictions only if atomic diffusion processes are moderated by turbulent mixing of moderate efficiency. We infer an intial cluster lithium abundance $\log \varepsilon(\mathrm{Li}) = 2.57 \pm 0.10$, which agrees with WMAP-calibrated BBN predictions, $\log \varepsilon(\mathrm{Li}) = 2.71 \pm 0.06$.

Key words. diffusion — globular clusters: individual (NGC 6397) — stars: abundances — stars: evolution — stars: fundamental parameters

1. Introduction

It is well known by now that the surface composition in old unevolved stars does not necessarily represent the initial composition (see e.g. Korn et al. 2007; Lind et al. 2008, 2009; González Hernández et al. 2009; Meléndez et al. 2010). Such variations are qualitatively predicted by stellar models taking into account the various effects commonly termed atomic diffusion: gravitational settling, radiative levitation, and thermal diffusion. Effects calculated from first principles are however consistently too strong, and only find quantiative agreement with observations when moderated by some ad-hoc description of turbulent mixing (Richard et al. 2002, 2005; Richard 2012).

In old, unevolved stars, gravitational settling is expected to redistribute most metals from the surface to below the convection zone. The magnitude of this effect depends on the interplay with the other processes. Evolving along the subgiant branch, the onset of the first dredge-up returns the settled material to the surface, so that surface abundances represent the initial composition. By comparing pre- and post-dredge-up abundances, the influence of turbulent mixing can be determined. Lithium however is destroyed by proton capture already at temperatures of 2.5×10^6 K. Its post-dredge-up surface abundance is not representative of the initial composition, which must instead be inferred from theoretical modeling.

In the stellar models of Richard et al. (2005) with effects of atomic diffusion and turbulent mixing of weak efficiency, roughly 0.2 dex of lithium is depleted from the surface layers of unevolved stars. Not all of this material is destroyed, but instead deposited below the convection zone. As the star evolves (to a stage here termed SGB), the convection zone deepens enough that deposited material resurfaces, increasing the surface abundance – forming a lithium abundance peak. Deeper yet, layers where lithium has been depleted are reached, and the surface lithium is diluted by the familiar dredge-up of lithium-poor material.

From detailed analyses of stars ranging from just past the main-sequence turnoff point (TOP), to below the red giant branch (RGB) in the metal-poor globular cluster NGC 6397 ([Fe/H ≈ -2.1), the independent analyses of Korn et al. (2007, hereafter Paper I) and Lind et al. (2008) determined significant evolutionary variations in surface abundances.

In Paper I, 3σ abundance variations in iron and magnesium were identified, along with weak variations in calcium and titanium. Additionally, a TOP–SGB lithium abundance peak of 0.14 ± 0.07 dex was found. This effect, as well as the TOP–RGB evolution of surface abundances in the four other chemical elements strongly suggested a moderate turbulent-mixing efficiency, at an assumed cluster age of 13.5 Gyr.

2. New analyses, new results

We have recently updated the analysis of Paper I. An in-depth presentation of our methods and details is given elsewhere (Nordlander et al. 2012). Briefly, we analyze a total of 18 stars grouped into four evolutionary stages. We identify an evolutionary iron abundance variation significant on the 3σ level, which is robust to the choice of temperature scale. We detect less significant variations in five other elements. We find that the previously preferred moderate turbulent-mixing efficiency models still best describe the behavior of all six elements. The evolution of lithium abundances for our TOP–SGB stars is strongly incompatible with predictions from the highly efficient turbulent mixing preferred by others in this cluster (González Hernández et al. 2009) as well as in the field (Meléndez et al. 2010). The optimal model indicates an initial lithium abundance of $\log \varepsilon(\mathrm{Li}) = 2.57 \pm 0.10$, which compares well with the WMAP-calibrated prediction $\log \varepsilon(\mathrm{Li}) = 2.71 \pm 0.06$ (Cyburt et al. 2010).

3. New fundamental parameters

The temperature scale of Paper I was based upon Hα wing broadening, yielding temperatures largely consistent with then current IRFM calibrations of both narrow- and broadband indices. Results were consistent both internally and on the absolute scale.

The photometric calibration on the IRFM for dwarfs and subgiants by Casagrande et al. (2010) indicates a systematic increase in surface temperatures by 100 K over previous calibrations. For our TOP stars, we see the exact same tendency of ~100 K higher temperatures. As this difference stems largely from the absolute calibration of infrared magnitudes into fluxes, the effect should be an absolute shift for all stars, including giants.

We account for these new results by increasing the Hα-based temperatures of each star in our sample by 100 K. This yields temperatures which have the internal precision of our detailed, homogeneous Hα analysis, and the absolute accuracy of the new IRFM determinations.

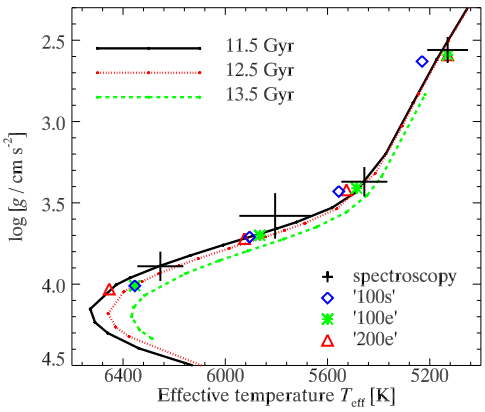

Fig. 1. Comparison of the group-averaged fundamental parameters of our stars to theoretical predictions. The spectroscopic determinations with error bars of Paper I are shown as crosses. Parameters on three different temperature scales are shown with colored symbols. The temperature scale presented here, '100s', agrees well with predictions for a cluster age of ∼12 Gyr. From left to right, we refer to these groups as the TOP, SGB, bRGB and RGB.

In Paper I, surface gravities were determined from the iron ionization equilibrium in NLTE. We depart from this by instead adopting photometry-based surface gravities. These are determined from observed V-magnitudes, estimates of the cluster's distance modulus and reddening excess, temperature-sensitive bolometric corrections, and theoretical stellar masses. Absolute values are sensitive to both distance and reddening. The internal precision on the other hand is very good, as it is not very sensitive to such systematics, nor to the measurement uncertainties.

As is shown in Figure 1, the combination of our new $T_{\rm eff}$ and $\log g$ values is consistent with theoretical predictions for a cluster of the expected age 12.0 ± 0.5 Gyr (Kowalski 2007). It is also consistent with the observed photometric cluster morphology, which indicates a temperature difference of 100–200 K between the turnoff point and our TOP stars.

4. New abundances

Armed with a new temperature scale, we have redetermined the abundances of five chemical elements: lithium, magnesium, calcium, titanium and iron. We have also determined chromium abundances.

Lithium, magnesium, calcium and chromium are all analyzed under NLTE. Abundances of titanium and iron are determined from ionic lines. For this reason, they are not very sensitive to neither NLTE effects nor temperatures. They are instead sensitive to the accuracy and precision of $\log g$. Our redetermined abundances of these elements are not significantly different from Paper I. In iron, the abundance difference $\Delta \log \varepsilon$(Fe)(RGB − TOP) = 0.16 ± 0.05 is significant on the 3σ level.

The calcium lines are sensitive to both temperature and surface gravity. The combined effect of altering these two parameters increases the abundance difference between the RGB and TOP stars somewhat, although the variation remains only mildly significant (Δ = 0.11 ± 0.07 dex).

Lithium abundances are now evaluated under NLTE. For the TOP stars, this cancels the effect of the increased temperature, giving abundances $\log \varepsilon$(Li) = 2.26 ± 0.10. This value is compatible with what we determine for the representative field halo star HD 84937, $\log \varepsilon$(Li) = 2.25, indicating no significant abundance difference between field and cluster stars. A lithium abundance peak is still identified on the SGB, although weaker than in Paper I, now indicating $\Delta \log \varepsilon$(Li)(SGB − TOP) = 0.12 ± 0.07.

We have determined sodium abundances in the bulk of our sample, and compare these to literature values (Lind et al. 2011) in Figure 2. A Mg-Na anticorrelation is identified – at 95 % probability by Kendall's τ test, with slope −0.53 ± 0.19 dex per dex – and corrected for among the RGB stars. As no first generation stars are identified in the other groups, we estimate the magnitude of this effect from the sodium abundances and increase the uncertainties in abundance determinations accordingly.

An insignificant Li-Na anticorrelation is seen among the RGB stars, indicating a tenta-

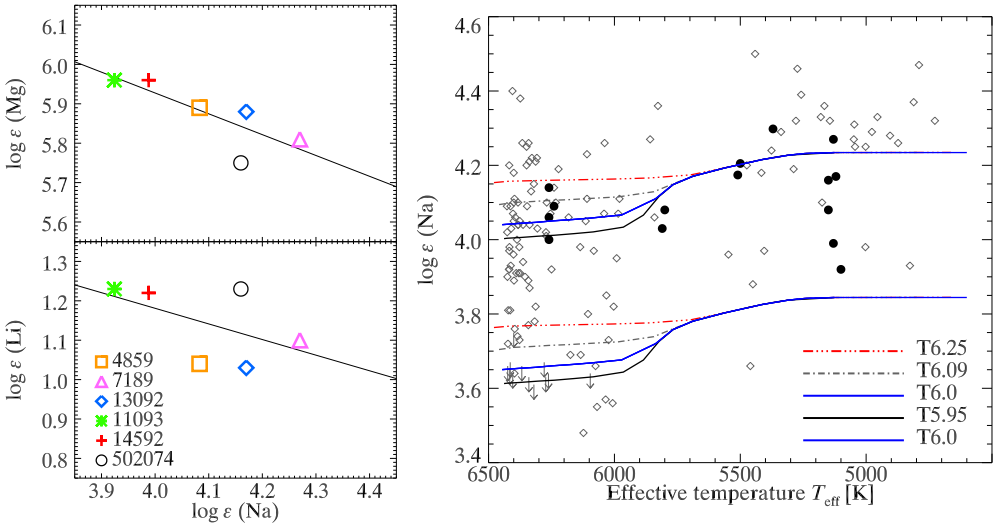

(a) Observed anticorrelations. (b) Sodium abundances compared to literature values.

Fig. 2. **(a)** Observed Mg-Na and Li-Na anticorrelations among the sample of six RGB stars. Each star, identified by an ID, is represented by a specific symbol and color. The separation between first and second generation RGB stars lies at roughly $\log \varepsilon(\mathrm{Na}) = 4.0$. First generation stars have the lower sodium abundances. **(b)** Our sodium abundances (black bullets) compared to survey data from Lind et al. (2011) (faint diamonds for detections, arrows for upper limits). The two sets of theoretical isochrones represent the first and second generations of stars in that work. Among our 18 stars, only the RGB group seems to contain any first-generation stars.

tive ∼0.1 dex difference between first and second generation stars at this evolutionary stage. As expected (Lind et al. 2009), no significant Li-Na anticorrelation is seen among our TOP stars.

5. New models

In Paper I, abundance variations were compared to predictions from theoretical models with weak-to-moderate efficiency of turbulent mixing, at an assumed age of 13.5 Gyr.

Since then, work on determining the white dwarf cooling sequence (WDCS) has lead to a precise age determination of 12.0 ± 0.5 Gyr (Kowalski 2007). A lower cluster age leaves less time for atomic diffusion to work, which should lead to flatter abundance trends. But a lower age also requires stars of a given evolutionary stage to be more massive. This leads to thinner convection zones, which allows more efficient atomic diffusion. These two effects partially cancel, and the precise age turns out not to be decisive for the magnitude of abundance variations.

Other groups have determined variations in lithium abundances tied to evolutionary state in NGC 6397 (González Hernández et al. 2009) or mass and metallicity in the field (Meléndez et al. 2010), which require modeling at a rather high efficiency of turbulent mixing (T6.25).

In Figure 3, we compare group-average abundances to predictions from theoretical models at an age compatible with results from the WDCS. Turbulent mixing efficiencies range from moderate to strong.

The predicted behavior varies between elements. Magnesium and iron simply settle below the surface convection zone. On the subgiant branch, the dredge-up recovers the inital composition. Lithium initially behaves similarly, until the dredge-up reaches depleted matter, which dilutes the surface abundance. A combination of radiative levitation and gravi-

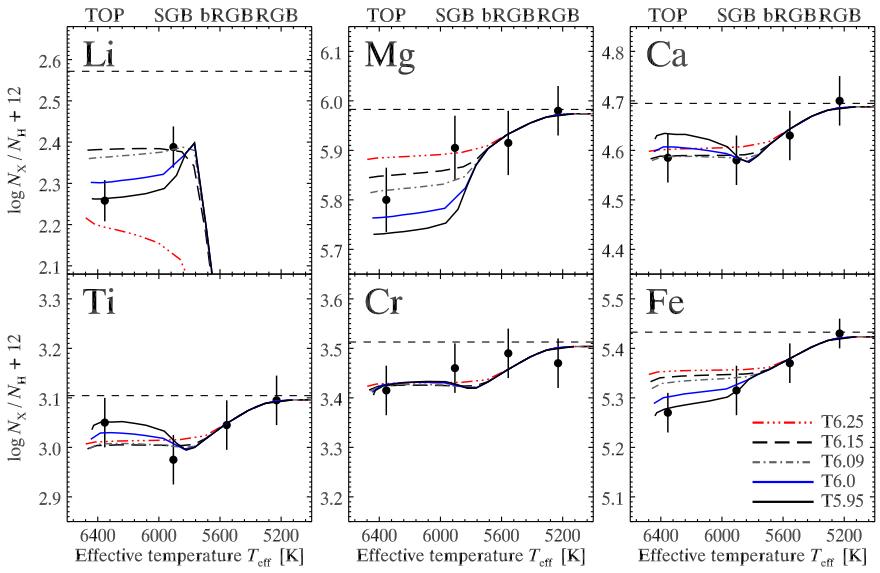

Fig. 3. Group-average abundances in six chemical elements on the new temperature scale. Results are compared to a 12.5 Gyr isochrone with five different efficiencies of turbulent mixing. The models T5.95–6.25 represent moderate to strong mixing. The optimal model is T6.0. The initial composition is indicated by horizontal dashed lines.

tational settling produces an inversion in the radial abundance profile of calcium, titanium, and to lesser degree, chromium. The dredge-up thus initially reduces these surface abundances via dilution, before they are restored to their initial values.

The opposite sensitivity of these two effects, and the very good correspondence to observations of six chemical elements with widely different parameter sensitivity indicates that the models in fact mimic reality, and that the results are not simply artefacts of e.g. the temperature scale or spurious NLTE or 3D effects.

The abundance analysis favors a moderate turbulent-mixing efficiency, with T6.0 the optimal model. The high-efficiency T6.25 model preferred by other groups disagrees with the observed TOP–RGB abundance variation in iron (by 2σ) and with the TOP–SGB variation in lithium (by 4σ).

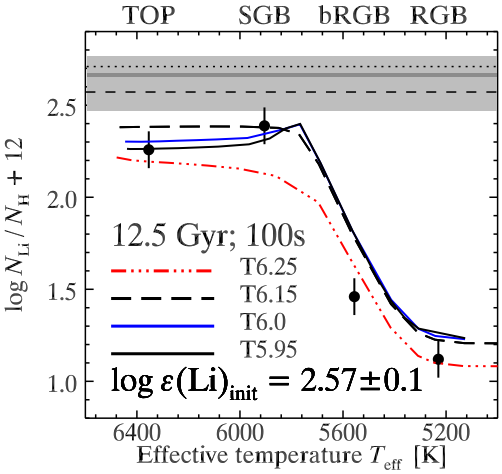

Fig. 4. Observed group-average lithium abundances compared to model predictions. The dashed and dotted lines correspond to the inferred initial cluster lithium abundance and the predicted primordial BBN value.

6. The initial lithium abundance

In Figure 4, the observed lithium abundances are compared to model predictions. From the globally favored model, T6.0, we infer an intial lithium abundance of $\log \varepsilon(\mathrm{Li})_{\mathrm{init}} = 2.57 \pm 0.1$, which agrees rather well with the WMAP-calibrated BBN prediction $\log \varepsilon(\mathrm{Li})_{\mathrm{prim}} = 2.71 \pm 0.06$ (Cyburt et al. 2010).

The absolute lithium abundance level of the models is determined from the abundances of the TOP and SGB stars. The high lithium abundances of the SGB stars strongly suggest a moderate efficiency of turbulent mixing, which leads to a rather strong (0.1 dex) over-prediction of lithium abundances in the RGB stars. On the other hand, a $\sim$0.1 dex first/second generation effect may be hiding in our RGB star abundance determinations – recall Figure 2.

Only by choosing to reject the SGB stars from this comparison could the unevolved TOP and the evolved RGB stars be found to agree on a model, and thus predict the same initial lithium composition. Curiously, such a solution would lessen the disagreement with the highly efficient turbulent-mixing model T6.25. Calibrating this model on the TOP and RGB star abundances would indicate a somewhat higher initial lithium abundance than was quoted above. This is due to the additional destruction of lithium caused by the deep turbulent mixing in such models.

Thus, regardless if one accepts the SGB lithium-peak (independently identified in NGC 6397 by Lind et al. 2009), the inferred initial lithium abundance is compatible with BBN predictions.

7. Conclusions

Our abundance analysis reaffirms the reality of atomic diffusion effects in metal-poor stars. Predicted abundance variations match observations well in six chemical elements, allowing us to determine the most likely effects on surface lithium abundances. From a set of preferred models implementing turbulent mixing of moderate efficiency, we determine an initial cluster lithium abundance of $\log \varepsilon(\mathrm{Li})_{\mathrm{init}} = 2.57 \pm 0.1$, which is compatible with BBN predictions.

Only by ignoring the atomic diffusion-induced increase in surface lithium abundances in stars just entering the subgiant branch, observed both here and elsewhere, do we find agreement with predictions from the highly efficient turbulent mixing preferred by others. Curiously, this scenario does not significantly change the inferred intial lithium abundance.

Finally, in a more general context, we do not detect a difference in lithium abundances between our least evolved cluster stars and the corresponding representative field halo star HD 84937. The initial lithium abundances inferred from cluster stars should thus be directly comparable with those from analyses of field stars, save for possible anti-correlations induced by cluster-internal pollution (Pasquini et al. 2005).

Acknowledgements. We wish to thank Luca Casagrande and Maria Bergemann for their valuable input.

References

Casagrande, L., Ramírez, I., Meléndez, J., Bessell, M., & Asplund, M. 2010, A&A, 512, A54

Cyburt, R. H., Ellis, J., Fields, B. D., et al. 2010, JCAP, 10, 32

González Hernández, J. I., Bonifacio, P., Caffau, E., et al. 2009, A&A, 505, L13

Korn, A. J., Grundahl, F., Richard, O., et al. 2007, ApJ, 671, 402

Kowalski, P. M. 2007, A&A, 474, 491

Lind, K., Charbonnel, C., Decressin, T., et al. 2011, A&A, 527, A148

Lind, K., Korn, A. J., Barklem, P. S., & Grundahl, F. 2008, A&A, 490, 777

Lind, K., Primas, F., Charbonnel, C., Grundahl, F., & Asplund, M. 2009, A&A, 503, 545

Meléndez, J., Casagrande, L., Ramírez, I., et al., 2010, A&A, 515, L3

Nordlander, T., Korn, A. J., Richard, O., & Lind, K. 2012, ApJ, in press. arXiv:1204.5600

Pasquini, L., Bonifacio, P., Molaro, P., et al. 2005, A&A, 441, 549

Richard, O. 2012, MSAIS, 22, 211

Richard, O., Michaud, G., & Richer, J. 2005, ApJ, 619, 538

Richard, O., Michaud, G., Richer, J., et al. 2002, ApJ, 568, 979